Caecilian Genomes Reveal the Molecular Basis of Adaptation and Convergent Evolution of Limblessness in Snakes and Caecilians

Vladimir Ovchinnikov,[1,†] Marcela Uliano-Silva ⬤,[2,†] Mark Wilkinson,[3] Jonathan Wood,[2]
Michelle Smith,[4] Karen Oliver,[4] Ying Sims,[2] James Torrance,[2] Alexander Suh,[5,6]
Shane A. McCarthy ⬤,[2,7] Richard Durbin ⬤,[2,7,*] and Mary J. O'Connell ⬤[1,*]

[1]Computational and Molecular Evolutionary Biology Group, School of Life Sciences, Faculty of Medicine and Health Science, University of Nottingham, Nottingham, United Kingdom

[2]Tree of Life Programme, Wellcome Sanger Institute, Cambridge, United Kingdom

[3]Herpetology Laboratory, The Natural History Museum, London, United Kingdom

[4]Scientific Operations, Wellcome Sanger Institute, Cambridge, United Kingdom

[5]School of Biological Sciences, University of East Anglia, Norwich, United Kingdom

[6]Department of Organismal Biology, Science for Life Laboratory, Uppsala University, Uppsala, Sweden

[7]Department of Genetics, University of Cambridge, Cambridge, United Kingdom

*Corresponding authors: E-mails: Mary.O'Connell@nottingham.ac.uk, rd109@cam.ac.uk.

[†]These authors contributed equally to this work.

Associate editor: Dr. Katja Nowick

Abstract

We present genome sequences for the caecilians *Geotrypetes seraphini* (3.8 Gb) and *Microcaecilia unicolor* (4.7 Gb), representatives of a limbless, mostly soil-dwelling amphibian clade with reduced eyes, and unique putatively chemosensory tentacles. More than 69% of both genomes are composed of repeats, with retrotransposons being the most abundant. We identify 1,150 orthogroups that are unique to caecilians and enriched for functions in olfaction and detection of chemical signals. There are 379 orthogroups with signatures of positive selection on caecilian lineages with roles in organ development and morphogenesis, sensory perception, and immunity amongst others. We discover that caecilian genomes are missing the zone of polarizing activity regulatorysequence (ZRS) enhancer of Sonic Hedgehog which is also mutated in snakes. In vivo deletions have shown ZRS is required for limb development in mice, thus, revealing a shared molecular target implicated in the independent evolution of limblessness in snakes and caecilians.

Key words: Gymnophiona, amphibia, vertebrate comparative genomics, limblessness.

Introduction

Living amphibians, frogs, salamanders, and caecilians, have diverged since the Triassic. They, or their ancestors, survived all mass extinctions including the Permian-Triassic which obliterated most terrestrial vertebrates (Wake and Vredenburg 2008). Our current extinction crisis places amphibians amongst the most threatened of the vertebrate groups (Blaustein and Wake 1990). In addition, the large and highly repetitive genomes typical in amphibia pose some of the greatest challenges for vertebrate genomics (Funk et al. 2018; Nowoshilow et al. 2018). Undoubtedly, reference quality genomes for amphibia will be important in addressing key aspects of their conservation, disease ecology and evolution, and breeding programs.

Caecilians (Gymnophiona) are the deepest diverging of the three extant amphibian orders and the sister group of the frogs and salamanders (Batrachia), diverging perhaps more than 300 million years ago (Siu-Ting et al. 2019). Compared to batrachians, caecilians are few in number (approximately 215 species). With mostly secretive burrowing lifestyles and restricted distributions in the wet tropics west of Wallace's line, they are relatively seldom encountered and often considered to be the least well-known group of tetrapods (Wilkinson 2012).

Caecilians are highly distinctive in their elongate (from 10 to 2 month adult lengths), and externally segmented snake- or worm-like form. Living species lack any trace of limbs or girdles, have skulls that are comparatively heavily ossified compared to batrachians, and have very short tails or no tails at all, all features that are associated with the fossorial or burrowing habits of adults. Eyes are also greatly reduced with any loss of vision seemingly compensated for by a putative chemosensory pair of tentacles on the

Open Access

snout that are not found in any other taxa (Taylor 1968; Wilkinson 2012). Other unique features include a dual-jaw closing mechanism, a copulatory organ formed from the hind part of the gut (phallodeum), and persistent Mullerian ducts in males. Their scientific name Gymnophiona means "naked snakes" reflecting their perceived affinity to snakes albeit without scales. Ironically, some caecilians do have subdermal scales (quite different from the external scales of squamates) concealed in pockets or folds in the skin and are the only living amphibians to have scales. Like most other amphibians, caecilians are generalist predators as adults (Measey et al. 2004; Wilkinson 2012).

As with other living amphibians, oviparity with an aquatic larval stage and metamorphosis to a terrestrial adult is the ancestral reproductive mode within the group. Clutches of relatively few eggs are laid on land rather than in water, entailing a migration to water for any hatchling-larvae, and are invariably guarded until hatching by attending mothers. Other reproductive strategies include oviparity with direct terrestrial development and viviparity. Foetuses of at least some viviparous caecilians are believed to use specialized teeth to feed on the hypertrophied and lipidified oviduct linings of their mothers and it was discovered that in some oviparous direct developers, their hatchlings feed on the similarly modified maternal epidermis with similarly specialized vernal teeth (Kupfer et al. 2006; Wilkinson et al. 2013). Caecilian diversity is far from completely known and most of the described species are data deficient in the International Union for Conservation of Nature (IUCN) red list and thus, lack any assessment of their conservation status and threats. New higher taxa (families and genera) have been recently discovered and caecilian species are described every year (Kamei et al. 2012; Wilkinson et al. 2021). Although many aspects of caecilian biology remain to be adequately investigated, phylogenetic relationships of the ten currently recognized families are reasonably well-established, and support the generally accepted idea that caecilians are an ancient Gondwanan group with relatively recent and limited dispersals into Central America and South East Asia (Gower et al. 2002; Kamei et al. 2012).

The Rhinatrematidae, the deepest diverging (c. 125 million year ago) of the ten caecilian families (Wilkinson et al. 2011), is represented by the only previously published caecilian genome Rhinatremata bivittatum, which is 5.3 Gb in size and was sequenced by the vertebrate genomes project (VGP) (Rhie et al. 2021). Here we provide reference quality genomes for two additional caecilian genomes, Geotrypetes seraphini (3.8 Gb) and Microcaecilia unicolor (4.7 Gb), and describe molecular level insights gleaned from their comparison with other vertebrate genomes.

Reference Genomes

The reference genomes of G. seraphini (Dermopdiidae) and M. unicolor (Siphonopidae) were assembled using four data types including Pacbio continuous long reads (CLR) and Hi-C reads, 10× Chromium linked-reads, and

BioNano optical maps (supplementary table S1, Supplementary Material online) and meet the VGP's 6.7.P5.Q40.C90 metric standards, the same used previously for Rhinatrema bivittatum and other vertebrates (Rhie et al. 2021). G. seraphini and M. unicolor, respectively, presented: contig N50 of 20.6 Mb and 3.6 Mb; scaffold N50 of 272 Mb and 376 Mb; and, Phred-scaled base accuracy Q43 and Q37 with 99% and 97% of sequences assigned to 19 and 14 chromosomes (table 1). Chromosomal units were identified and named by size (fig. 1). The final assembly sizes were 3.8 Gb and 4.7 Gb, respectively (table 1). Manual curation was performed as in Howe et al. (2021) (supplementary fig. S1, Supplementary Material online) resulting in 69 and 55 removals of misjoins, 122 and 84 new joins, and 18 and 0 removals of false duplications for G. seraphini and M. unicolor, respectively.

A synteny analyses performed with single-copy Benchmarking Universal Single-Copy Orthologs (BUSCO) genes shows that chromosome content and gene order are conserved to a remarkable extent across caecilian chromosomes, with large blocks of collinear synteny up to chromosome-scale further conserved to anurans (common frog and toad) across more than 600 million years of evolution (fig. 2).

Repeat Content

Substantial proportions of the caecilian genomes were found to consist of repeats: a total of 67.7%, 72.5%, and 69.3% for R. bivittatum (Rhie et al. 2021), G. seraphini and M. unicolor, respectively (supplementary table S2, Supplementary Material online). Class I transposable elements (TEs; retrotransposons) are ~20 times more abundant (in base pairs) than Class II TEs (DNA transposons) and make up more than 30% of each caecilian genome. Long interspersed elements (LINEs) are the most abundant transposon type, followed by dictyostelium intermediate repeat sequences (DIRSs), that is tyrosine recombinase retroelements. These relative proportions differ from those found in the large genomes of other amphibians including caecilians; for example, a genomic low-coverage shotgun analysis of the caecilian Ichthyophis bannanicus (genome size 12.2 Gb) revealed more DIRSs than LINEs (Wang et al. 2021), while published salamander genomes are dominated by long terminal repeat (LTR) elements, with DIRSs never surpassing 7% of their content (Sun and Mueller 2014; Nowoshilow et al. 2018). These findings bolster the concept that repeated extreme TE accumulation in amphibians is not resulting from failure to control a specific type of TE (Wang et al. 2021).

Gene Family Analyses

Comparing the protein-coding regions of the three caecilian genomes across 22 vertebrate genomes we identified a set of 31,385 orthogroups, of which 15,216 contained caecilian genes. We identified 265 gene families present across vertebrates but missing in amphibia, and an additional 260 orthogroups lost specifically in caecilians (supplementary
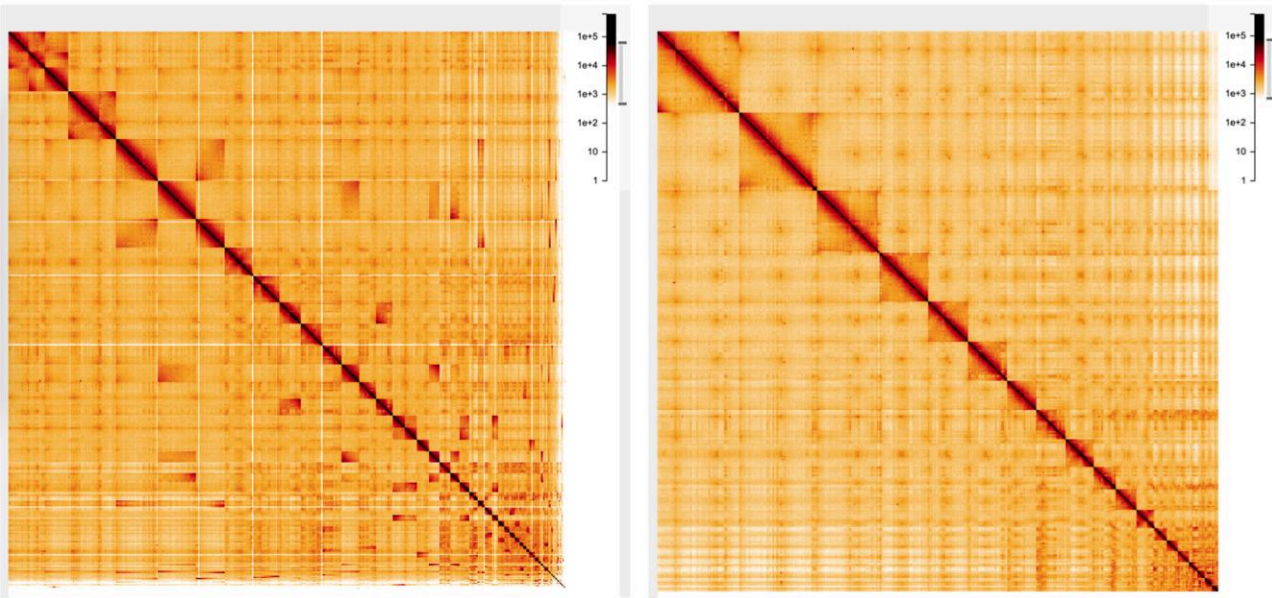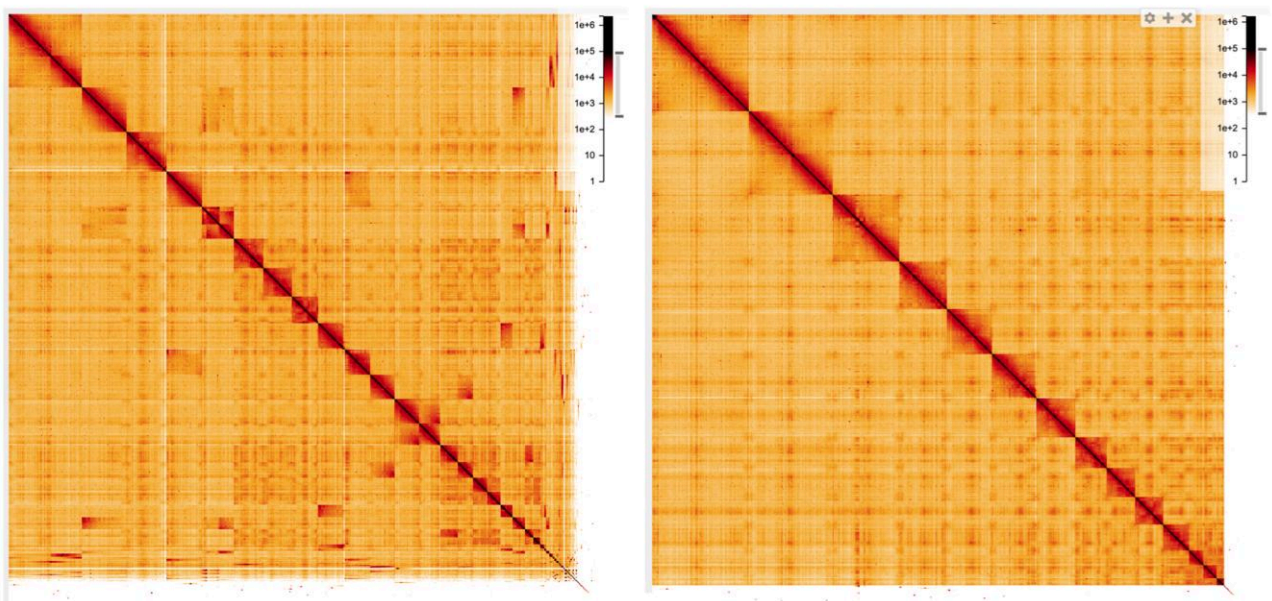
Geotrypetes seraphini Hi-C heatmaps before (left) and after (right) manual curation

Microcaecilia unicolor Hi-C heatmaps before (left) and after (right) manual curation

Fɪɢ. 1. *Geotrypetes seraphini* and *Microcaecilia unicolor* genome Hi-C contact maps, respectively. The contact maps show Hi-C reads at 8.192 Mb resolution in HiGlass. The top two panels are *G. seraphini* and the bottom two panels are *M. unicolor* and, in both cases, the left panel is before and the right panel is after manual curation. Chromosomes are ordered from large (left/top) to small (right/bottom). After the VGP Assembly Pipeline and manual curation, 99.8% and 97% of sequences were assigned to 19 and 14 chromosomes for *G. seraphini* and *M. unicolor*, respectively.

table S3, Supplementary Material online). In contrast, 1,150 orthogroups are present only in caecilians (supplementary table S4, Supplementary Material online) and are enriched for functions such as olfaction and detection of chemical signals (*P*-value < 0.01). At least 20% of these caecilian-specific genes contained one of three protein domains (zf-C$_2$H$_2$, Krüppel-associated box (KRAB), 7tm_4). The 7tm_4 proteins are transmembrane olfactory receptors (Buck and Axel 1991); enrichment of this domain amongst the novel protein families in caecilians suggests an intense

selective pressure on chemosensory perception at the origin of the caecilians, as they adapted to life underground with reduced vision and compensatory elaboration of chemosensory tentacles. Proteins containing zf-C2H2 and KRAB domains are known to have functions in regulating transcription, with zf-C$_2$H$_2$-containing proteins in humans shown to recognize more motifs than any other transcription factor family. In addition, KRAB and zf-C2H2-containing proteins have been shown to bind currently active and ancient families of specific TEs (e.g., LINEs

and LTRs/endogenous retrovirus [ERVs]) (Najafabadi et al. 2015). The emergence of novel gene families with these functional capacities at the origin of caecilians may have contributed to the unique pattern of TE accumulation we observe in this group; further work is needed.

We performed a gene birth and death analysis using CAFE v5 (Mendes et al. 2020) on the remaining 13,541 orthogroups, examining the ancestral and extant caecilian nodes where possible. The majority of these (10,035) orthogroups had no net change in gene family size between caecilian species and the ancestral amphibian node (8,065 orthogroups) or had insufficient sampling (1,970 orthogroups), and were excluded from further analysis. We reconstructed ancestral states for the remaining 3,506 orthogroups (supplementary table S5, Supplementary Material online). There were 156 orthogroups that were completely absent in G. seraphini and M. unicolor (most likely lost in their most recent common ancestor) (supplementary table S3, Supplementary Material online). Only 13 orthogroups showed significant changes in the number of caecilians (fig. 3, supplementary table S6, Supplementary Material online), with five expansions at the ancestral caecilian node (ACN), and three at the internal caecilian node (ICN), of which one gene family is significantly expanded at both nodes. There are a total of three gene families with significant contractions, all of which are on the ACN. The gene families displaying significant expansions are: cytochrome P450 family 2 (ACN), these monooxygenases catalyze many reactions involved in the metabolism of a large number of xenobiotics and endogenous compounds (Manikandan and Nagini 2018); butyrophilin (BTN) family (ACN), involved in milk lipid secretion in lactation and regulation of the immune response (Afrache et al. 2012); tripartite motif (TRIM) family (ACN and ICN) involved in a broad range of biological processes that are associated with innate immunity (Ozato et al. 2008); and H2A and H2B histones (ICN), which
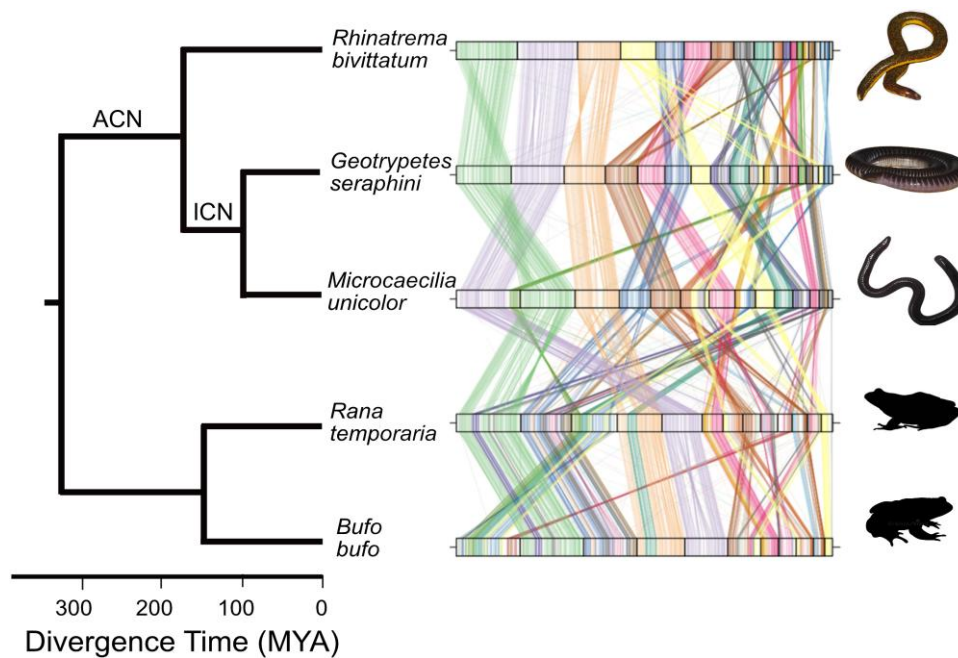
Table 1. Final Genome Assembly Statistics for *Geotrypetes Seraphini* and *Microcaecilia Unicolor*.

Species (ID)	Geotrypetes seraphini (aGeoSer1)	Microcaecilia unicolor (aMicUni1)
Assembly Length	3,779,430,017	4,685,939,421
sequence assigned to chromosomes	99.84%	97.05%
Number of Contigs	597	3530
Contig N50	20,656,571	3,661,507
Number of Scaffolds	164	1081
Scaffold N50	272,612,222	376,147,139
Scaffolds assigned to chromosomes	19	14
Assembly quality value	43	37
BUSCO (vertebrata_odb10)	C:95.3%[S:92.8%, D:2.5%], F:2.5%,M:2.2%, n:3354	C:95.5%[S:91.7%, D:3.8%], F:2.4%,M:2.1%, n:3354
NCBI accession	GCA_902459505.2	GCA_901765095.2

FIG. 2. Synteny plots showing the conservation of large-scale gene linkage and gene order across caecilians, and to a substantial extent across amphibia. Conserved unique single-copy vertebrate genes were identified with BUSCO and connected by lines according to their chromosomal location in *Rhinatrema bivittatum*. TheACN andICN are labeled. Common frog *Rana temporaria* and toad *Bufo bufo* genomes from https://wellcomeopenresearch.org/articles/6-286 and https://wellcomeopenresearch.org/articles/6-281, respectively. Synteny was identified with ChrOrthLink (https://github.com/chulbioinfo/chrorthlink). Images of caecilians are modified (with permission) using the Gimp software from original photos taken by Mark Wilkinson. Frog and toad silhouettes are taken from http://phylopic.org/.
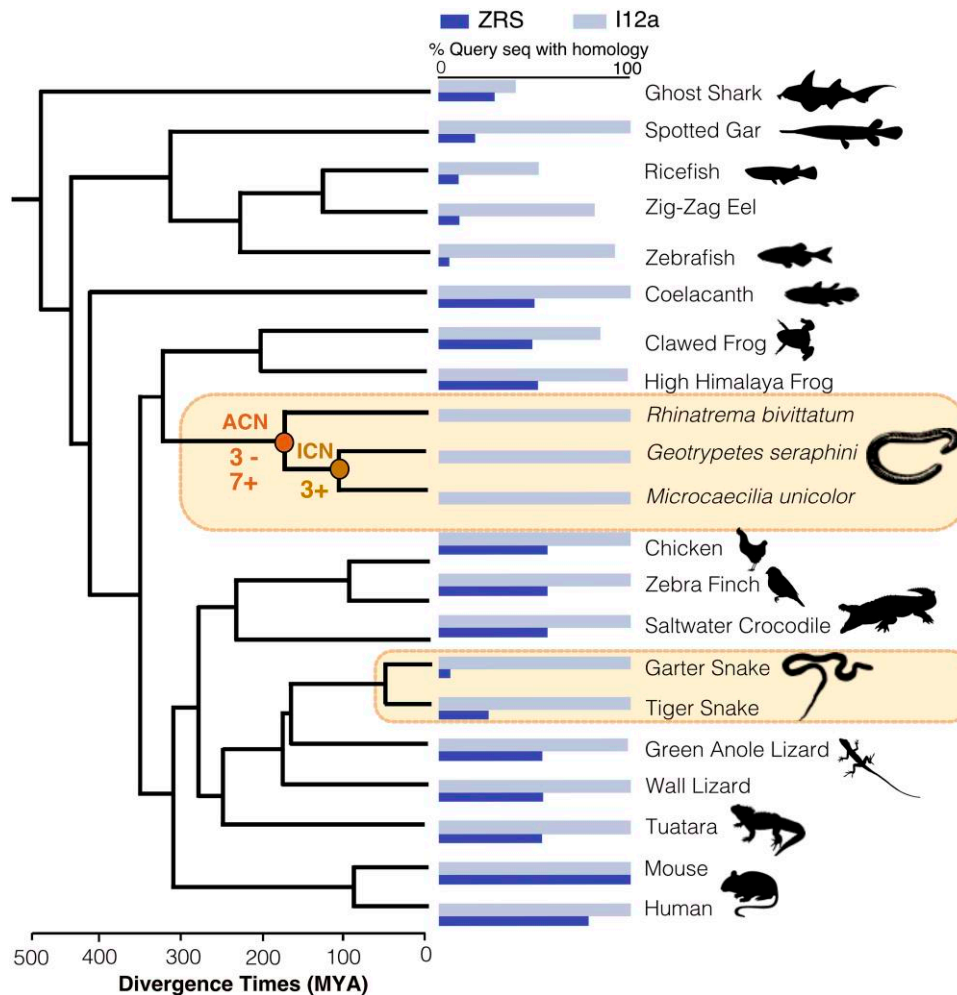
Fig. 3. Summary of sequence conservation of two enhancer elements across vertebrates (ZRS and I12a). The vertebrate species phylogeny used throughout this study is shown on the left with the significant gene gain and loss events noted on the ancestral and internal caecilian nodes (ACN and ICN), respectively. The histogram shows the level of sequence conservation identified by BLASTN for each species for two enhancers: I12a (pale shaded bars) and ZRS (dark shaded bars). Snakes and caecilians are highlighted as they independently evolved limbless morphologies. Animal images are taken from http://phylopic.org/.

together with H3 and H4 histones and DNA form a nucleosome (Koyama and Kurumizaka 2018). In contrast, while immune function-related BTN and TRIM families have significant expansions at the ACN and/or ICN, both immunoglobulin heavy and light variable gene families have significant contractions at the ACN. The final gene family displaying significant contractions is gamma crystallin, a structural protein found largely in the nuclear region of the lens of the eye at very high concentrations (Vendra et al. 2016). Changes in these gene family repertoires may have contributed to the transition to a fossorial lifestyle and the packaging of a large genome.

Identification of Genes With Signatures of Positive Selection

Variation in selective pressure was assessed using codon-based models of evolution to assess changes in dN/dS across sites and lineages as implemented in codeml in

the PAML package (Yang 2007). All 1,935 gene families that reached our criteria (see Materials and Methods) were analyzed. These 1,935 gene families were functionally enriched for Gene Ontology (GO) terms "extracellular structure organization", "developmental process", "regulation of biological process", "response to stress", "cell communication", "signal transduction", "regulation of signaling", and "leukocyte differentiation" (supplementary table S7, Supplementary Material online). The lineages specified as foreground were the branch leading to the extant caecilians (ACN), and all terminal and internal branches within the caecilian clade. The selective pressures, that is positive or negative selection or neutral evolution, were estimated for each gene within each foreground lineage and were compared to all other vertebrates (background lineages) in the alignment. Here we report the signatures of positive selection (dN/dS > 1) identified in homologs on the foreground (i.e., caecilian) lineages. After Bonferroni correction, we detected 379 orthologous families with evidence of caecilian

lineage-specific positive selective pressure (supplementary table S8, Supplementary Material online). We did not find any statistical enrichment for GO functions in the genes under positive selection on the nodes tested. Examples of genes with signatures of positive selection on the ACN are FBN1 (under positive selection on both the ACN and the ICN), AGTPBP1, and CEP290 all of which are involved in eye morphogenesis (Chakrabarti et al. 2006; Sheck et al. 2018; Stephenson et al. 2020). Genes with signatures of positive selection on the ICN include: Thrombomodulin (THBD) (involved in the reduction of thrombin), Wnt ligand secretion mediator (WLS) (enables Wnt-protein binding activity and is involved in several processes, including animal organ development; mesoderm formation; and positive regulation of canonical Wnt signaling pathway), and CD8A (mediates efficient cell–cell interactions within the immune system). In addition, collagen COL3A1 is under positive selection on all caecilian nodes tested (i.e., ACN, ICN, and terminal nodes). A sample of the genes under positive selection within specific caecilian lineages are described as follows (specific internal caecilian lineage in parenthesis): HESX1 (*R. bivittatum*) required for the normal development of the forebrain, eyes, and other anterior structures such as the olfactory placodes and pituitary gland (Dattani et al. 1998); NFE2L2 (*G. seraphini*), a transcription factor that plays a key role in the response to oxidative stress (Huang et al. 2000; Eggler et al. 2009; Huppke et al. 2017; Sanghvi et al. 2019); LGR4 (*R. bivittatum*) is involved in the development of the anterior segment of the eye (Siwko et al. 2013) and is required for the development of various organs, including kidney, intestine, skin, and reproductive tract (Hoshii et al. 2007; Kinzel et al. 2014); COL9A3 (*M. unicolor*) encodes a component of Collagen IX —a structural component of cartilage, intervertebral discs and the vitreous body of the eye (Olsen 1997; He and Karsdal 2016). In summary, whilst the biological processes and functions of the genes under positive selection are not significantly enriched, there are several genes implicated in organ (especially eye) development and morphogenesis. Caecilian tentacles can be considered as compensation for reduced vision through enhanced olfaction, and they are thought to be materially related (by transformation) to components of the visual system such as eyelids and lacrimal ducts (Billo and Wake 1987). Therefore, a tentative explanation for the positive selection we observe on genes associated with organ (eye) development and morphogenesis is the origin of the tentacles from ancestral visual components. The approach we have taken in our analysis of selective pressure variation is necessarily stringent, and, therefore, not a complete assessment of the entire genome where there are likely many other processes at work.

Analysis of ZRS Enhancer Loss

Some key enhancers for developmental regulator genes are very strongly conserved at the sequence level across all vertebrates. For example, the I12a enhancer element, located between homeobox genes Dlx1 and Dlx2, is known to be conserved from bony fish to mice (Plessy et al. 2005).

Analysis of the ortholog of the I12a enhancer across the 22 vertebrate species confirms that it is easily identifiable and conserved in all vertebrates, including the three caecilians (fig. 3). Similarly, the ZRS enhancer element for the Sonic hedgehog gene (Shh), which is located within an intron of the LMBR1 gene, is almost ubiquitously conserved in vertebrates. However, snakes contain a mutant form of ZRS that when placed into mice produces a "serpentised" phenotype, directly implicating loss of ZRS function in vertebrate limblessness (Kvon et al. 2016). From the fossil record, we know that snake limblessness pre-dates that of limbless lizards, also reflected in a higher level of divergence in limb regulatory elements in snakes in comparison to limbless lizards. Indeed, ZRS is intact in limbless lizards where more complex and lineage-specific routes to limblessness have been proposed (Roscito et al. 2022). Here we show that the conserved ZRS element is absent (or mutated beyond recognition) in the three caecilian genomes. Specifically, there is no trace of homology by sequence matching (fig. 3), and a conserved ETS1 binding site within the ZRS enhancer element, which has been shown to be critical for limb development in mouse and is missing in snakes (Lettice et al. 2012; Kvon et al. 2016), is also entirely missing in caecilians (supplementary fig. S2, Supplementary Material online). Combined with the functional work on the mutated form of the snake ZRS, this may provide us with a potential common molecular target implicated in the convergent loss of limbs in snakes and caecilians. Alternatively, the observed pattern of loss of the ZRS element in caecilians could be secondary to the loss of limbs. Similar to the situation in lizards (Roscito et al. 2022), the loss of limbs in caecilians could have been piecewise and relaxation of selective pressures on the ZRS region could have resulted in its eventual loss from caecilian genomes. Functional analysis will be needed to finally resolve the history of limb loss in this major amphibian group.

Materials and Methods

Sample Preparation and Genome Assembly

Genome sequences were produced from wild-caught animals that had been maintained in captivity for several years. Specimens are at the Natural History Museum, London cataloged under their unique field tags: *G. seraphini* (MW11051) from Kon, Cameroon, and *R. bivittatum* (MW11052) and *M. unicolor* (MW11053), both from Camp Patawa, Kaw Mountains, French Guiana. All DNA extractions were from liver tissue using the Bionano Animal Tissue Plug preparation (https://bionanogenomics.com/wp-content/uploads/2018/02/30077-Bionano-Prep-Animal-Tissue-DNA-Isolation-Soft-Tissue-Protocol.pdf). Pacific Biosciences libraries were prepared with the Express Template Prep Kit 1.0 and Blue Pippin size selected. Pacific Biosciences CLR data was generated from 36 SMRTcells of *M. unicolor* and six SMRTcells of *G. seraphini* sequenced with the S/P2-C2/5.0 sequencing chemistry on the Pacific Biosciences Sequel

machine. A further 5 SMRTcells of *G. seraphini* were sequenced with S/P3-C1/5.0-8 M sequencing chemistry on a Pacific Biosciences Sequel II machine. The Hi-C libraries were created with a Dovetail Hi-C kit for *G. seraphini* and an Arima Genomics kit (version 1) for *M. unicolor* and sequenced on an Illumina HiSeq X. A 10× Genomics Chromium machine was used to create the linked-read libraries which were sequenced on an Illumina HiSeq X. Optical maps were created for both species using a Bionano Saphyr instrument. Raw reads statistics and data access links are available in supplementary table S1, Supplementary Material online.

Assembly for *G. seraphini* and *M. unicolor* was conducted mainly for *R. bivittatum* as described in (Rhie et al. 2021) using four data types and the VGP assembly pipeline (version 1.6 for *G. seraphini* and version 1.5 for *M. unicolor*; supplementary fig. S1, Supplementary Material online). In brief, the Pacific Biosciences CLR data for each species was input to the diploid-aware long-read assembler FALCON and its haplotype-resolving tool FALCON-UNZIP (Chin et al. 2016). The resulting primary and alternate assemblies of *M. unicolor* were input to Purge Haplotigs (Roach et al. 2018) and *G. seraphini* assemblies were input to Purge_dups (Guan et al. 2020) for identification and removal of remaining haplotigs. Both species' primary assemblies were subject to two rounds of scaffolding using 10× long molecule linked-reads and Scaff10× (https://github.com/wtsi-hpag/Scaff10X), and one round of Bionano Hybrid-scaffolding with pre-assembled Cmaps from 1-enzyme non-nicking (direct labelling enzyme [DLE]-1) and the Solve Pipeline. The resulting scaffolds were then further scaffolded into chromosome-scale scaffolds using the Dovetail/Arima library Hi-C data for *G. seraphini*/*M. unicolor* and SALSA2 (Ghurye et al. 2019). The scaffolded primary assemblies plus the Falcon-phased haplotigs were then subjected to Arrow (Chin et al. 2013) polishing with the Pacbio reads and two rounds of short read polishing using the 10× Chromium linked-reads, longranger align (Bishara et al. 2015), freebayes (Garrison and Marth 2012) and consensus calling with bcftools (Danecek et al. 2021) (further details available in Rhie et al 2021, and supplementary fig. S1, Supplementary Material online). Assemblies were checked for contamination and were manually curated using gEVAL system (Chow et al. 2016), HiGlass (Kerpedjiev et al. 2018), and PretextView (https://github.com/wtsi-hpag/PretextView) as described previously (Howe et al. 2021). Mitochondria were assembled using mitoVGP (Formenti et al. 2021). Manual curation was performed as described by Howe et al. (2021). Genome annotation was carried out using the NCBI Eukaryotic Genome Annotation Pipeline, which produces homology-based and ab initio gene predictions to annotate genes (including protein-coding and noncoding as lncRNAs, snRNAs), pseudo-genes, transcripts, and proteins (https://www.ncbi.nlm.nih.gov/genbank/eukaryotic_genome_submission_annotation/). Caecilian annotations available on NCBI at the accessions GCF_902459505.1, GCF_901765095.1 are summarized in supplementary table S9, Supplementary Material online. Raw reads statistics, accession numbers and software versions employed can be found in supplementary table S1, Supplementary Material online.

Prediction and annotation of repeats were achieved using a de novo library of repeats generated with RepeatModeler2 for each species (Flynn et al. 2020), combined with the Repbase "Amphibia" library (release 26.04) (Bao et al. 2015) to form the final library for each species. Repeats were masked with RepeatMasker (http://www.repeatmasker.org/) and Window Masker (Morgulis et al. 2006). Then transcripts, proteins, and RNA-Seq from the NCBI database were aligned to the genomes using Splign (Kapustin et al. 2008) and ProSplign (https://www.ncbi.nlm.nih.gov/sutils/static/prosplign/prosplign.html). Alignments were submitted to Gnomon (https://www.ncbi.nlm.nih.gov/genome/annotation_euk/gnomon/) for gene prediction. Models built on RefSeq transcript alignments were given preference over overlapping Gnomon models with the same splice pattern. Supplementary table S2, Supplementary Material online presents a summary of caecilian repeat annotations. RepeatModeler libraries in fastA format are available from DOI:10.5281/zenodo.7540729.

Data Assembly and Treatment for the Comparative Study

Coding DNA sequences (CDSs) for 21 vertebrate species (supplementary fig. S3, Supplementary Material online) were downloaded from Ensembl release 100 (Yates et al. 2020). In those cases where a more contemporary version of the genome was available on RefSeq (Release 200) (O'Leary et al. 2016) we used the RefSeq genome and corresponding annotations (supplementary Supplementary, Supplementary Material online supplementary table S10, Supplementary Material online). The longest canonical protein-coding region for each gene was retained for further analysis.

Orthogroup Prediction and Gene Birth and Death Analysis

We identified 31,385 orthogroups for the 419,877 protein-coding regions across 21 vertebrate species using OrthoFinder (Emms and Kelly 2019) (all orthogroups are available at DOI:10.5281/zenodo.7540729). We used a phylostratigraphic approach to explore caecilian-specific losses in the context of the uncontroversial vertebrate phylogeny used throughout (fig. 3), which we extracted from timetree.org (Kumar et al. 2017) assembled from the following literature: caecilians (Mauro et al. 2014), amphibians (Siu-Ting et al. 2019), fish (Betancur-R et al. 2017), reptiles (Pyron et al. 2013), mammals (Morgan et al. 2013; Tarver et al. 2016), and birds (Chiari et al. 2012). The phylogenetic distribution of the orthogroups revealed 1,150 that were gained in caecilians, and 525 that were absent in all three caecilians. Information about species-specific losses elsewhere in the tree was not carried forward for further analysis. We partitioned the orthogroups that lack

caecilian representation in the following ways: (1) to identify orthogroups that lack representation across all amphibia: we identified orthogroups that contained at least two fish species and two tetrapod (nonamphibian) species—totalling 265 orthogroups, (2) to identify orthogroups that are absent only in caecilians: we extracted those orthogroups with least two fish species and two tetrapod species (including at least one frog species)—totalling 238 orthogroups, (3) to identify orthogroups that are present across amphibia and amniota but absent in caecilians: we extracted orthogroups containing two frog species and two amniota species—totalling 22 orthogroups. Orthogroups that did not contain caecilian sequences and that did not satisfy these filters were set aside. Combining the set of orthogroups that contain caecilian representatives (13,541) plus those that passed our filters 1–3 above (525), produced our final set of 14,066 orthogroups for analysis in CAFE v5 with Poisson distribution option and the lambda parameter (rate of change of evolution) estimated for each species (Mendes et al. 2020). All 3,506 orthogroups showing expansions or contractions within caecilians are provided in supplementary table S5, Supplementary Material online, and orthogroups with significant expansions and contractions are detailed in supplementary table S6, Supplementary Material online.

Analysis of Selective Pressure Variation

Our selective pressure variation analysis focussed on 3,236 single-copy orthogroups (single gene ortholog [SGOs]) and 9,690 multicopy genes (MCGs) from our orthogroups. The 9,690 MCGs obtained from the CAFE analysis, could be further broken down into SGO clusters as follows: 3,464 contained species-specific duplications in a single lineage, and were designated SGOs by removal of the single lineage containing the duplications; the remaining 6,226 were divided into their constituent single-copy paralogous groups using UPhO (Ballesteros and Hormiga 2016). Species-specific gene duplications that were not specific to caecilians were removed. In total, this provided 14,807 SGOs (3,236 original SGOs plus 11,571 SGOs generated from MCGs) for further analysis. We used three different alignment methods on the amino-acid sequences for these SGOs (i.e., MAFFT (Rozewicki et al. 2019) (with –auto option), MUSCLE (Edgar 2004), and Prank (Löytynoja 2014) (with -nobppa option)), and used MetAl (Blackburne and Whelan 2012) to assess the statistical significance of the resultant alignments. If the difference between alignments was ≥5%, the alignment with the highest NorMD (Thompson et al. 2001) score was used. The corresponding gene trees were reconstructed using IQtree (Nguyen et al. 2015) (with 100 bootstraps for each tree and models of best fit selected on a gene-by-gene basis). Robinson-Foulds distances between each of the gene trees generated and the canonical species tree were estimated using Clann (Creevey and McInerney 2005), and only those gene trees with zero distance were retained for further

analysis, that is the gene and species tree were required to be in full agreement thus, minimizing the risk of hidden paralogy in our single-copy gene orthogroups (SGOs). It has been shown that codeml provides more accurate predictions when a minimum of seven species are present in the dataset (Anisimova et al. 2002), gene families that did not meet this criterion were not considered for selective pressure variation analysis. We assessed the patterns of selective pressure variation on the remaining 1,935 SGOs using codon-based models of evolution in codeml (Yang 2007) using our pipeline for large-scale analyses "Vespasian" (Constantinides et al. 2021). The models we employed are a set of standard nested models which are automatically compared by Vespasian using likelihood ratio tests with significance calculated using the appropriate degrees of freedom. The models used were the neutral model M1Neutral, its lineage-specific extensions model A, and the null model for model A. M1Neutral allows two site classes for dN/dS (referred to as ω throughout): $\omega 0 = 0$ and $\omega 1 = 1$. Model A assumes the two site classes are the same in both foreground and background lineages ($\omega 0 = 0$ and $\omega 1 = 1$) and $\omega 2$ for the foreground is estimated from the data and free to vary above 1. Model A null estimates a $\omega 2$ value also, but here it is restricted to below 1 thus, allowing sites to be evolving under either purifying selection or to be neutrally evolving but not permitting positive selection. Sequences were considered to exhibit lineage-specific selective pressure if the likelihood ratio test for ModelA is significant in comparison to both ModelA null and M1Neutral. All alignments (codon-based and amino-acid) for the selective pressure analyses are available at DOI:10.5281/zenodo.7540729. The GO terms were predicted for all caecilian CDSs using eggNOG with "orthology restrictions" option set to "transfer annotations from one-to-one orthology only" (eggnog-mapper.embl.de) (Huerta-Cepas et al. 2019) and all other parameters as default. GO term enrichment analysis was carried out using goatools (Klopfenstein et al. 2018) with Taxonomic Scope auto-adjusted per query.

Comparative Analysis of the ZRS Enhancer

The ZRS enhancer sequence is located within an intron between exons 5 and 6 of the mouse LMBR1 gene sequence (Gene ID: 105804842) (Kvon et al. 2016). The LMBR1 sequence was extracted from the genomes of each species in our sample set (supplementary table S11, Supplementary Material online) and the homologous intron sequence containing the ZRS sequence was identified across all species. Using BLASTn (Camacho et al. 2009) the ZRS region was readily identifiable across all 22 noncaecilian species (fig. 3, and supplementary fig. S2, Supplementary Material online) but was not detectable in the three caecilian genomes. The ZRS sequence was also searched against the reference genome assemblies of all three caecilians (to account for possible relocation of the enhancer) and we did not identify a ZRS-like sequence in an alternative location in the caecilian genomes. Using the

same approach, we quantified the level of sequence conservation across our set of vertebrates for an additional enhancer, I12a (AF349438.2), located between the homeobox bigene cluster paralogs DLX1 and DLX2 (supplementary table S11, Supplementary Material online). The DLX1 gene was not annotated for Crocodylus porosus, therefore, we used the region between METAP1D and DLX2.

Supplementary material

Supplementary data are available at *Molecular Biology and Evolution* online, the genomes for *G. serephini* and *M. unicolor* are available from NCBI via accession numbers GCA_902459505.2 and GCA_901765095.2 respectively. All processed data files used in the analyses described above are available from https://doi.org/10.5281/zenodo.7540729.

Acknowledgments

Author Contributions

M.W. supplied all biological samples and contributed to the interpretation of results. M.S. performed DNA extractions and optical mapping. K.O. coordinated the creation of sequencing libraries and genomic sequencing. S.A.M. generated the genome assemblies. Y.S., J.T., and J.W. performed the manual curation of the assemblies. M.U.S. performed BUSCO synteny analyses and with AS the repeat analyses. M.J.O.'C. and V.O. performed and interpreted the selective pressure analyses and birth and death analyses. M.J.O.'C. and V.O. carried out the comparative analysis of ZRS and I12a enhancer elements and interpreted the results. R.D. supervised the genomics aspects of the project and M.J.O.'C. the comparative analyses. All authors contributed to writing the manuscript.

References

Afrache H, Gouret P, Ainouche S, Pontarotti P, Olive D. 2012. The butyrophilin (BTN) gene family: from milk fat to the regulation of the immune response. *Immunogenetics.* **64**:781–794.

Anisimova M, Bielawski JP, Yang Z. 2002. Accuracy and power of Bayes prediction of amino acid sites under positive selection. *Mol Biol Evol.* **19**:950–958.

Ballesteros JA, Hormiga G. 2016. A new orthology assessment method for phylogenomic data: unrooted phylogenetic orthology. *Mol Biol Evol.* **33**:2117–2134.

Bao W, Kojima KK, Kohany O. 2015. Repbase update, a database of repetitive elements in eukaryotic genomes. *Mob DNA.* **6**:11.

Betancur-R R, Wiley EO, Arratia G, Acero A, Bailly N, Miya M, Lecointre G, Ortí G. 2017. Phylogenetic classification of bony fishes. *BMC Evol Biol.* **17**:162.

Billo R, Wake MH. 1987. Tentacle development in dermophis mexicanus (amphibia, Gymnophiona) with an hypothesis of tentacle origin. *J Morphol.* **192**:101–111.

Bishara A, Liu Y, Weng Z, Kashef-Haghighi D, Newburger DE, West R, Sidow A, Batzoglou S. 2015. Read clouds uncover variation in complex regions of the human genome. *Genome Res.* **25**:1570–1580.

Blackburne BP, Whelan S. 2012. Measuring the distance between multiple sequence alignments. *Bioinformatics.* **28**:495–502.

Blaustein AR, Wake DB. 1990. Declining amphibian populations: a global phenomenon? *Trends Ecol Evol.* **5**:203–204.

Buck L, Axel R. 1991. A novel multigene family may encode odorant receptors: a molecular basis for odor recognition. *Cell.* **65**:175–187.

Camacho C, Coulouris G, Avagyan V, Ma N, Papadopoulos J, Bealer K, Madden TL. 2009. BLAST+: architecture and applications. *BMC Bioinformatics.* **10**:421.

Chakrabarti L, Neal JT, Miles M, Martinez RA, Smith AC, Sopher BL, La Spada AR. 2006. The purkinje cell degeneration 5J mutation is a single amino acid insertion that destabilizes nna1 protein. *Mamm Genome.* **17**:103–110.

Chiari Y, Cahais V, Galtier N, Delsuc F. 2012. Phylogenomic analyses support the position of turtles as the sister group of birds and crocodiles (archosauria). *BMC Biol.* **10**:65.

Chin C-S, Alexander DH, Marks P, Klammer AA, Drake J, Heiner C, Clum A, Copeland A, Huddleston J, Eichler EE, et al. 2013. Nonhybrid, finished microbial genome assemblies from long-read SMRT sequencing data. *Nat Methods.* **10**:563–569.

Chin C-S, Peluso P, Sedlazeck FJ, Nattestad M, Concepcion GT, Clum A, Dunn C, O'Malley R, Figueroa-Balderas R, Morales-Cruz A, et al. 2016. Phased diploid genome assembly with single-molecule real-time sequencing. *Nat Methods.* **13**:1050–1054.

Chow W, Brugger K, Caccamo M, Sealy I, Torrance J, Howe K. 2016. gEVAL - a web-based browser for evaluating genome assemblies. *Bioinformatics.* **32**:2508–2510.

Constantinides B, Orr D, Ovchinnikov V, Mulhair P, Webb AE, O'Connell MJ. 2021. Vespasian: genome scale detection of selective pressure variation (Version 0.5.3) [Computer software]. *GitHub.* https://doi.org/10.5281/zenodo.5779868.

Creevey CJ, McInerney JO. 2005. Clann: investigating phylogenetic information through supertree analyses. *Bioinformatics.* **21**:390–392.

Danecek P, Bonfield JK, Liddle J, Marshall J, Ohan V, Pollard MO, Whitwham A, Keane T, McCarthy SA, Davies RM, et al. 2021. Twelve years of SAMtools and BCFtools. *GigaScience.* **10**:giab008.

Dattani MT, Martinez-Barbera JP, Thomas PQ, Brickman JM, Gupta R, Mårtensson IL, Toresson H, Fox M, Wales JK, Hindmarsh PC, et al. 1998. Mutations in the homeobox gene HESX1/Hesx1 associated with septo-optic dysplasia in human and mouse. *Nat Genet.* **19**:125–133.

Edgar RC. 2004. MUSCLE: multiple sequence alignment with high accuracy and high throughput. *Nucleic Acids Res.* **32**:1792–1797.

Eggler AL, Small E, Hannink M, Mesecar AD. 2009. Cul3-mediated nrf2 ubiquitination and antioxidant response element (ARE) activation are dependent on the partial molar volume at position 151 of Keap1. *Biochem J.* **422**:171–180.

Emms DM, Kelly S. 2019. Orthofinder: phylogenetic orthology inference for comparative genomics. *Genome Biol.* **20**:238.

Flynn JM, Hubley R, Goubert C, Rosen J, Clark AG, Feschotte C, Smit AF. 2020. Repeatmodeler2 for automated genomic discovery of

transposable element families. *Proc Natl Acad Sci U S A.* **117**: 9451–9457.

Formenti G, Rhie A, Balacco J, Haase B, Mountcastle J, Fedrigo O, Brown S, Capodiferro MR, Al-Ajli FO, Ambrosini R, *et al.* 2021. Complete vertebrate mitogenomes reveal widespread repeats and gene duplications. *Genome Biol.* **22**:120.

Funk WC, Zamudio KR, Crawford AJ. 2018. Advancing understanding of amphibian evolution, ecology, behavior, and conservation with massively parallel sequencing. In: Hohenlohe PA and Rajora OP, editors. *Population genomics: wildlife. Population genomics*. Cham: Springer International Publishing. p. 211–254. Available from: https://doi.org/10.1007/13836_2018_61

Garrison E, Marth G. 2012. Haplotype-based variant detection from short-read sequencing. :Preprint at https://arxiv.org/abs/1207.3907.

Ghurye J, Rhie A, Walenz BP, Schmitt A, Selvaraj S, Pop M, Phillippy AM, Koren S. 2019. Integrating hi-C links with assembly graphs for chromosome-scale assembly. *PLoS Comput Biol.* **15**:e1007273.

Gower DJ, Kupfer A, Oommen OV, Himstedt W, Nussbaum RA, Loader SP, Presswell B, Müller H, Krishna SB, Boistel R, *et al.* 2002. A molecular phylogeny of ichthyophiid caecilians (Amphibia: Gymnophiona: Ichthyophiidae): out of India or out of South East Asia? *Proc R Soc B Biol Sci.* **269**:1563–1569.

Guan D, McCarthy SA, Wood J, Howe K, Wang Y, Durbin R. 2020. Identifying and removing haplotypic duplication in primary genome assemblies. *Bioinformatics.* **36**:2896–2898.

He Y, Karsdal MA. 2016. Chapter 9—type IX collagen. In: Morten AK Leeming DJ Henriksen K and Bay-Jensen A-C, editors. *Biochemistry of collagens, laminins and elastin : structure, function and biomarkers*: Academic Press. p. 67–71. Available from: https://doi.org/10.1016/C2015-0-05547-2

Hoshii T, Takeo T, Nakagata N, Takeya M, Araki K, Yamamura K. 2007. LGR4 Regulates the postnatal development and integrity of male reproductive tracts in mice. *Biol Reprod.* **76**:303–313.

Howe K, Chow W, Collins J, Pelan S, Pointon D-L, Sims Y, Torrance J, Tracey A, Wood J. 2021. Significantly improving the quality of genome assemblies through curation. *GigaScience.* **10**:giaa153.

Huang HC, Nguyen T, Pickett CB. 2000. Regulation of the antioxidant response element by protein kinase C-mediated phosphorylation of NF-E2-related factor 2. *Proc Natl Acad Sci U S A.* **97**:12475–12480.

Huerta-Cepas J, Szklarczyk D, Heller D, Hernández-Plaza A, Forslund SK, Cook H, Mende DR, Letunic I, Rattei T, Jensen LJ, *et al.* 2019. eggNOG 5.0: a hierarchical, functionally and phylogenetically annotated orthology resource based on 5090 organisms and 2502 viruses. *Nucleic Acids Res.* **47**:D309–D314.

Huppke P, Weissbach S, Church JA, Schnur R, Krusen M, Dreha-Kulaczewski S, Kühn-Velten WN, Wolf A, Huppke B, Millan F, *et al.* 2017. Activating de novo mutations in NFE2L2 encoding NRF2 cause a multisystem disorder. *Nat Commun.* **8**:818.

Kamei RG, Mauro DS, Gower DJ, Van Bocxlaer I, Sherratt E, Thomas A, Babu S, Bossuyt F, Wilkinson M, Biju SD. 2012. Discovery of a new family of amphibians from northeast India with ancient links to Africa. *Proc R Soc B Biol Sci.* **279**:2396–2401.

Kapustin Y, Souvorov A, Tatusova T, Lipman D. 2008. Splign: algorithms for computing spliced alignments with identification of paralogs. *Biol Direct.* **3**:20.

Kerpedjiev P, Abdennur N, Lekschas F, McCallum C, Dinkla K, Strobelt H, Luber JM, Ouellette SB, Azhir A, Kumar N, *et al.* 2018. Higlass: web-based visual exploration and analysis of genome interaction maps. *Genome Biol.* **19**:125.

Kinzel B, Pikiolek M, Orsini V, Sprunger J, Isken A, Zietzling S, Desplanches M, Dubost V, Breustedt D, Valdez R, *et al.* 2014. Functional roles of lgr4 and lgr5 in embryonic gut, kidney and skin development in mice. *Dev Biol.* **390**:181–190.

Klopfenstein DV, Zhang L, Pedersen BS, Ramírez F, Warwick Vesztrocy A, Naldi A, Mungall CJ, Yunes JM, Botvinnik O, Weigel M, *et al.* 2018. GOATOOLS: a python library for gene ontology analyses. *Sci Rep.* **8**:10872.

Koyama M, Kurumizaka H. 2018. Structural diversity of the nucleosome. *J Biochem (Tokyo).* **163**:85–95.

Kumar S, Stecher G, Suleski M, Hedges SB. 2017. Timetree: a resource for timelines, timetrees, and divergence times. *Mol Biol Evol.* **34**: 1812–1819.

Kupfer A, Müller H, Antoniazzi MM, Jared C, Greven H, Nussbaum RA, Wilkinson M. 2006. Parental investment by skin feeding in a caecilian amphibian. *Nature.* **440**:926–929.

Kvon EZ, Kamneva OK, Melo US, Barozzi I, Osterwalder M, Mannion BJ, Tissières V, Pickle CS, Plajzer-Frick I, Lee EA, *et al.* 2016. Progressive loss of function in a limb enhancer during snake evolution. *Cell.* **167**:633–642. e11.

Lettice LA, Williamson I, Wiltshire JH, Peluso S, Devenney PS, Hill AE, Essafi A, Hagman J, Mort R, Grimes G, *et al.* 2012. Opposing functions of the ETS factor family define shh spatial expression in limb buds and underlie polydactyly. *Dev Cell.* **22**:459–467.

Löytynoja A. 2014. Phylogeny-aware alignment with PRANK. *Methods Mol Biol Clifton NJ.* **1079**:155–170.

Manikandan P, Nagini S. 2018. Cytochrome P450 structure, function and clinical significance: a review. *Curr Drug Targets.* **19**:38–54.

Mauro DS, Gower DJ, Müller H, Loader SP, Zardoya R, Nussbaum RA, Wilkinson M. 2014. Life-history evolution and mitogenomic phylogeny of caecilian amphibians. *Mol Phylogenet Evol.* **73**:177–189.

Measey GJ, Gower DJ, Oommen OV, Wilkinson M. 2004. A subterranean generalist predator: diet of the soil-dwelling caecilian Gegeneophis ramaswamii (Amphibia; Gymnophiona; Caeciliidae) in southern India. *C R Biol.* **327**(1):65–76.

Mendes FK, Vanderpool D, Fulton B, Hahn MW. 2020. CAFE 5 Models variation in evolutionary rates among gene families. *Bioinformatics.* **36**:5516–5518.

Morgan CC, Foster PG, Webb AE, Pisani D, McInerney JO, O'Connell MJ. 2013. Heterogeneous models place the root of the placental mammal phylogeny. *Mol Biol Evol.* **30**:2145–2156.

Morgulis A, Gertz EM, Schäffer AA, Agarwala R. 2006. Windowmasker: window-based masker for sequenced genomes. *Bioinformatics.* **22**:134–141.

Najafabadi HS, Mnaimneh S, Schmitges FW, Garton M, Lam KN, Yang A, Albu M, Weirauch MT, Radovani E, Kim PM, *et al.* 2015. C2h2 zinc finger proteins greatly expand the human regulatory lexicon. *Nat Biotechnol.* **33**:555–562.

Nguyen L-T, Schmidt HA, von Haeseler A, Minh BQ. 2015. IQ-TREE: a fast and effective stochastic algorithm for estimating maximum-likelihood phylogenies. *Mol Biol Evol.* **32**:268–274.

Nowoshilow S, Schloissnig S, Fei J-F, Dahl A, Pang AWC, Pippel M, Winkler S, Hastie AR, Young G, Roscito JG, *et al.* 2018. The axolotl genome and the evolution of key tissue formation regulators. *Nature.* **554**:50–55.

O'Leary NA, Wright MW, Brister JR, Ciufo S, Haddad D, McVeigh R, Rajput B, Robbertse B, Smith-White B, Ako-Adjei D, *et al.* 2016. Reference sequence (RefSeq) database at NCBI: current status, taxonomic expansion, and functional annotation. *Nucleic Acids Res.* **44**:D733–D745.

Olsen BR. 1997. Collagen IX. *Int J Biochem Cell Biol.* **29**:555–558.

Ozato K, Shin D-M, Chang T-H, Morse HC. 2008. TRIM Family proteins and their emerging roles in innate immunity. *Nat Rev Immunol.* **8**:849–860.

Plessy C, Dickmeis T, Chalmel F, Strähle U. 2005. Enhancer sequence conservation between vertebrates is favoured in developmental regulator genes. *Trends Genet.* **21**:207–210.

Pyron RA, Burbrink FT, Wiens JJ. 2013. A phylogeny and revised classification of Squamata, including 4161 species of lizards and snakes. *BMC Evol. Biol.* **13**:93.

Rhie A, McCarthy SA, Fedrigo O, Damas J, Formenti G, Koren S, Uliano-Silva M, Chow W, Fungtammasan A, Kim J, *et al.* 2021. Towards complete and error-free genome assemblies of all vertebrate species. *Nature.* **592**:737–746.

Roach MJ, Schmidt SA, Borneman AR. 2018. Purge haplotigs: allelic contig reassignment for third-gen diploid genome assemblies. *BMC Bioinformatics.* **19**:460.

Roscito JG, Sameith K, Kirilenko BM, Hecker N, Winkler S, Dahl A, Rodrigues MT, Hiller M. 2022. Convergent and lineage-specific

genomic differences in limb regulatory elements in limbless reptile lineages. *Cell Rep.* **38**:110280.

Rozewicki J, Li S, Amada KM, Standley DM, Katoh K. 2019. MAFFT-DASH: integrated protein sequence and structural alignment. *Nucleic Acids Res.* **47**:W5–W10.

Sanghvi VR, Leibold J, Mina M, Mohan P, Berishaj M, Li Z, Miele MM, Lailler N, Zhao C, de Stanchina E, *et al.* 2019. The oncogenic action of NRF2 Depends on De-glycation by fructosamine-3-kinase. *Cell.* **178**:807–819.e21.

Sheck L, Davies WIL, Moradi P, Robson AG, Kumaran N, Liasis AC, Webster AR, Moore AT, Michaelides M. 2018. Leber congenital amaurosis associated with mutations in CEP290, clinical phenotype, and natural history in preparation for trials of novel therapies. *Ophthalmology.* **125**:894–903.

Siu-Ting K, Torres-Sánchez M, San Mauro D, Wilcockson D, Wilkinson M, Pisani D, O'Connell MJ, Creevey CJ. 2019. Inadvertent paralog inclusion drives artifactual topologies and timetree estimates in phylogenomics. *Mol Biol Evol.* **36**:1344–1356.

Siwko S, Lai L, Weng J, Liu M. 2013. Lgr4 in ocular development and glaucoma. *J Ophthalmol.* **2013**:987494.

Stephenson KAJ, Dockery A, O'Keefe M, Green A, Farrar GJ, Keegan DJ. 2020. A FBN1 variant manifesting as non-syndromic ectopia lentis with retinal detachment: clinical and genetic characteristics. *Eye.* **34**:690–694.

Sun C, Mueller RL. 2014. Hellbender genome sequences shed light on genomic expansion at the base of crown salamanders. *Genome Biol Evol.* **6**:1818–1829.

Tarver JE, Dos Reis M, Mirarab S, Moran RJ, Parker S, O'Reilly JE, King BL, O'Connell MJ, Asher RJ, Warnow T, *et al.* 2016. The interrelationships of placental mammals and the limits of phylogenetic inference. *Genome Biol Evol.* **8**:330–344.

Taylor EH. 1968. *The caecilians of the world: a taxonomic review.* Lawrence: University of Kansas Press.

Thompson JD, Plewniak F, Ripp R, Thierry JC, Poch O. 2001. Towards a reliable objective function for multiple sequence alignments. *J Mol Biol.* **314**:937–951.

Vendra VPR, Khan I, Chandani S, Muniyandi A, Balasubramanian D. 2016. Gamma crystallins of the human eye lens. *Biochim Biophys Acta.* **1860**:333–343.

Wake DB, Vredenburg VT. 2008. Are we in the midst of the sixth mass extinction? A view from the world of amphibians. *Proc Natl Acad Sci U S A.* **105**:11466–11473.

Wang J, Itgen MW, Wang H, Gong Y, Jiang J, Li J, Sun C, Sessions SK, Mueller RL. 2021. Gigantic genomes provide empirical tests of transposable element dynamics models. *Genomics Proteomics Bioinformatics.* **19**:123–139.

Wilkinson M. 2012. Caecilians. *Curr Biol.* **22**:R668–R669.

Wilkinson M, Reynolds RP, Jacobs JF. 2021. A new genus and species of rhinatrematid caecilian (Amphibia: Gymnophiona: Rhinatrematidae) from Ecuador. *Herpetol J.* **31**:27–34.

Wilkinson M, San Mauro D, Sherratt E, Gower DJ. 2011. A nine-family classification of caecilians (Amphibia: Gymnophiona). *Zootaxa.* **2874**:41–64.

Wilkinson M, Sherratt E, Starace F, Gower DJ. 2013. A new species of skin-feeding caecilian and the first report of reproductive mode in Microcaecilia (amphibia: Gymnophiona: Siphonopidae). *PLoS One.* **8**:e57756.

Yang Z. 2007. PAML 4: phylogenetic analysis by maximum likelihood. *Mol Biol Evol.* **24**:1586–1591.

Yates AD, Achuthan P, Akanni W, James A, Jamie A, Alvarez-Jarreta J, Amode MR, Armean IM, Azov AG, Bennett R, *et al.* 2020. Ensembl 2020. *Nucleic Acids Res.* **48**:D682–D688.